Control circuit of an Electronically Controlled Capacitor for the Optimization of the Single Phase Induction Motor

Radu Câmpeanu, Adrian Dănilă
Transilvania University of Brasov, Romania, radu.campeanu@unitbv.ro, adrian.danila@unitbv.ro

***Abstract* – The control circuit of an Electronically Controlled Capacitor (ECC) for the optimization of the Single Phase Induction Motor (SPIM) with auxiliary winding is presented. The control circuit is based on a fixed value AC capacitor within a full bidirectional switches bridge PWM controlled at much higher than line frequency (in kHz range). The power bridge circuit and its embedded pulse driver circuit are presented within the theoretical sections of the paper. In the experimental section, using a small electric motors test bench and a two speed SPIM with auxiliary winding, are analyzed the main influences of the pulse drive circuit over the ECC. Firstly, being considered that the optimum is reached at the maximum motor torque, the optimal pulses frequency has been established around 4 kHz. Secondly, the switches over-voltages at the commutations moments being a serious drawback of the ECC, are analyzed the influence of the fixed capacitor value and the dead time of the pulse shape over the MOS-FET power transistors of the bidirectional switches over-voltages. The over-voltages diminish as both the capacitor value and the dead time diminish. More than that, in contrast with some authors, there are no disadvantages as dead time became zero. These issues are the main contributions of this paper.**

Keywords: *Electronic Controlled Capacitor, Single Phase Induction Motors, PWM Control, Pulses Dead Time*.

I. INTRODUCTION

There are multiple methods to optimize induction motor regarding design, manufacturing process, driving or starting [1-5]. For single phase motor a promising method is to emulate a variable capacitor, starting from a fixed value capacitor. The usual way to electronically control a fixed value capacitor operating at the line frequency to obtain a so called Electronically Controlled Capacitor (ECC) is to switch the fixed value capacitor according to one of the three methods presented below.

A. The Liu-Muljadi method

The first is the Liu-Muljadi method [6, 7].

This method consists of an AC voltage capacitor directly commutated by a bidirectional switch connected in parallel with the capacitor (Fig. 1). The switch is closed in the moment the capacitor voltage is zero, ZVS (Zero Voltage Switching). The ECC is PWM controlled at line frequency.

The relation between the equivalent capacitance, C_e of the electronically commutated capacitor and the duty cycle of the control pulses is [6]:

$$C_e = \frac{C}{1-d} \tag{1}$$

where C is the capacitance of the fixed value capacitor and d is the duty cycle.

This method has the advantage of simplicity but an important disadvantage also, the distortions of the load current are high.

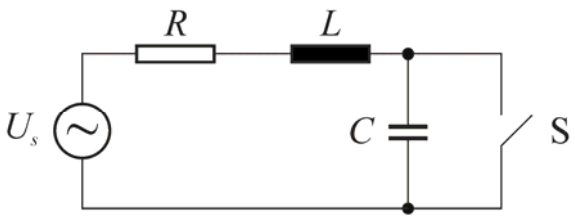

Fig. 1. The Liu - Muljadi method to emulate a variable capacitor.

B. The Lettenmaier method

The second method, proposed by T. A. Lettenmaier, consists of a DC charged capacitor inserted into a full controlled bridge. The commutation frequency provided by the PWM generator is in the range of some kHz, [8], Fig. 2.

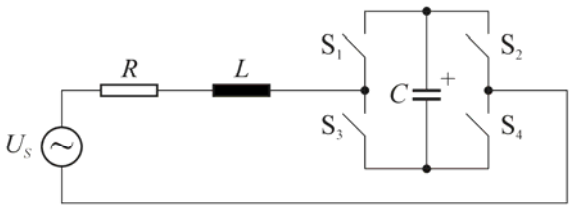

Fig. 2. The Lettenmaier method to emulate a variable capacitor.

C. The Suciu method

A similar but simpler method has been proposed by Suciu, [9-14], based on an AC voltage capacitor within a full controlled high frequency PWM bridge. This method has been adopted in our experiments.

The relation between the equivalent capacitance, C_e of the electronically commutated capacitor and the duty cycle of the control pulses is given by the following expression, [9]:

$$C_e = \frac{C}{(2 \cdot d - 1)^2} \quad (2)$$

where C is the capacitance of the fixed value capacitor and d is the duty cycle.

This ECC can modify the equivalent capacitance in the range from C - i. e. the fixed value of the AC capacitor (in the case the duty cycle is 0 or 1) - and theoretical infinity (if the duty cycle is ½). It can be observed that as the duty cycle increase from zero to unity the equivalent capacitance value of the ECC increase till value 1/2 of the duty cycle and then decrease as well.

II. The Power circuit

The power circuit is a full controlled bidirectional switches bridge. A bidirectional switching unit has two power MOS-FETs (IRFPG50PBF, 1000 V, 6.1 A, 1.5 Ω) in common control configuration and supplementary added freewheeling diodes (fast switching RHRP8120, 1200 V, 8 A), presented in Fig. 3 (electrical diagram) and Fig. 4 (experimental implementation).

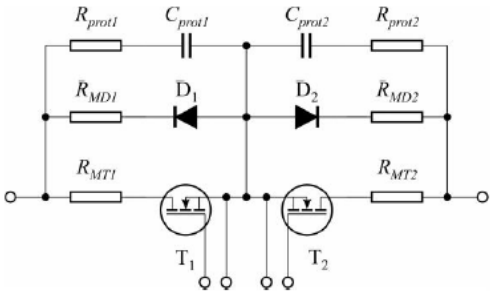

Fig. 3. Electrical diagram of the bidirectional switch.

The switching unit is provided with two RC protection groups and non-inductive resistors in order to evaluate the currents.

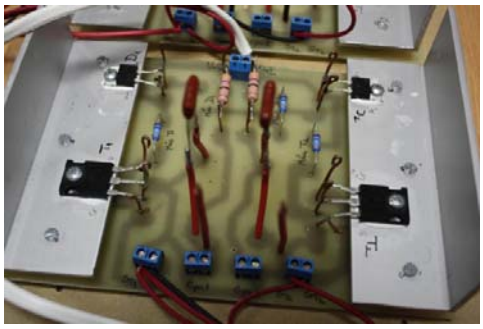

Fig. 4. The experimental implementation of a switching unit.

The electrical diagram of the full controlled power bridge circuit is presented in Figure 5.

A commutation cycle consists of two steps. For the positive polarity of the lower terminal of the bridge, in the first commutation step the transistors A_1, D_1 and the freewheeling diodes A_2, D_2 are switched on. In the second commutation step the transistors C_1, B_1 and the freewheeling diodes C_2, B_2 are switched on. For the negative polarity of the lower terminal of the bridge, in the first commutation step the transistors A_2, D_2 and the freewheeling diodes A_1, D_1 are switched on. In the second commutation step the transistors C_2, B_2 and the freewheeling diodes C_1, B_1 are switched on.

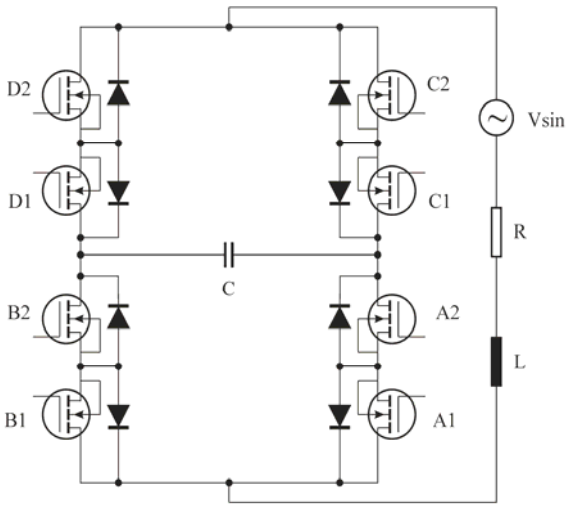

Fig. 5. Electrical diagram of the full controlled power bridge.

III. The Control circuit of power bridge

The control circuit of the power bridge has two sections (Fig. 6) an embedded PWM pulse generator and an opto-isolated drive circuit for the bidirectional switches of the bridge.

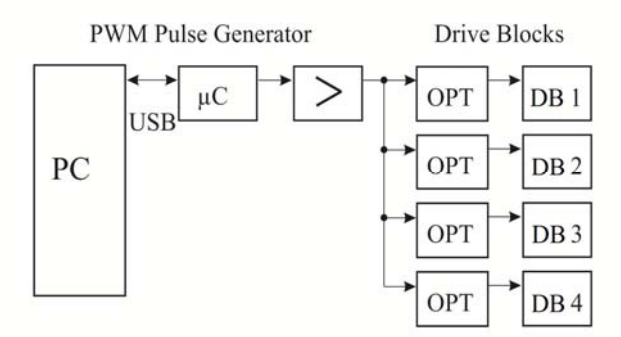

Fig. 6. The control circuit of the power bridge.

The first section is an Arduino Leonardo microcontroller PC controlled (via USB). It can generate pulses in a wide frequency and duty cycle ranges with variable dead time. The generator is followed by an amplifier to assure the optic-couplers current.

The second section consists of four drive blocks with specialized integrated circuits (power MOS-FETs drivers). The detailed electrical diagram of a drive block is presented in Figure 7.

This section is double isolated, once from the PWM pulse generator via eight high speed 6N137 optic-couplers and then from line by four line transformers (TR).

The main parts of a drive block are the isolation transformer, two floating DC voltage sources and two IR2117 power MOS-FET drivers.

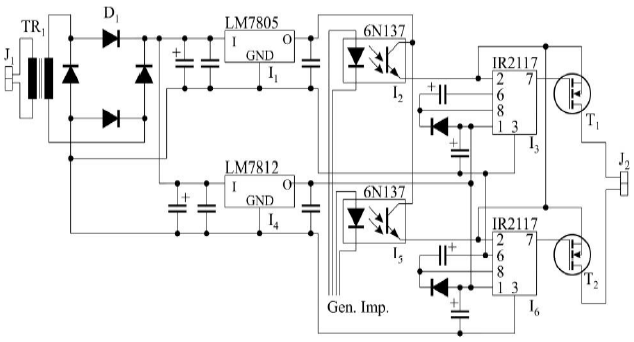

Fig. 7. The drive block electric diagram.

The output waveforms from optic-couplers are presented in Fig. 8.

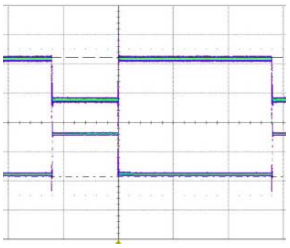

Fig. 8. The pulses forms.

In Fig. 9 is presented a detail with the dead time (here 1 µs).

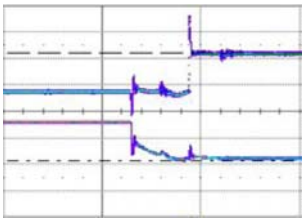

Fig. 9. The pulses dead time.

A detail of the output waveforms from drive block is presented in Fig. 10, transition time being about 0.5 µs.

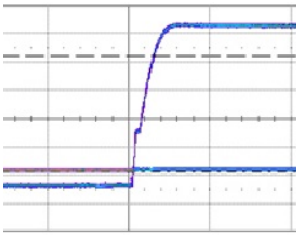

Fig. 10. The drive block output pulses transition.

IV. The Experimental Results

The control circuit has been integrated in a small motors measuring system [15-17].

In Fig. 11 is presented the structure of the system. It is composed by the Magtrol hysteresis dynamometer HD-805-8NA (DYN), the Magtrol brake controller DSP-6001 (CONTR), the motor coupling system (CS), the PC, the ECC and the line transformer (TR).

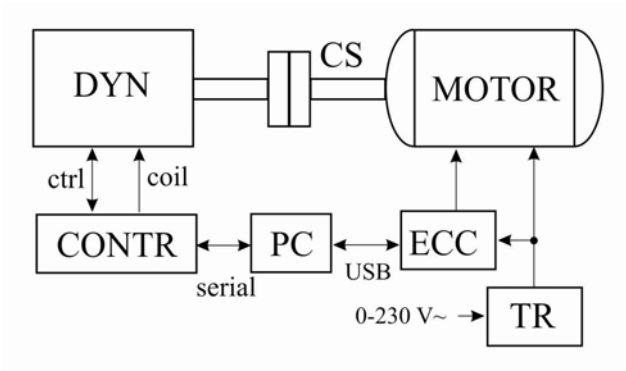

Fig. 11. Motor measuring system structure.

In Fig. 12 is presented the experimental setup. The motor and the dynamometer cannot be seen in this picture. The components of the experimental setup are the PC and the dynamometer controller (1), the transformer (2), the Arduino generator (3), the four driver blocks (4), the power bridge (9) and the fixed value capacitor (6).

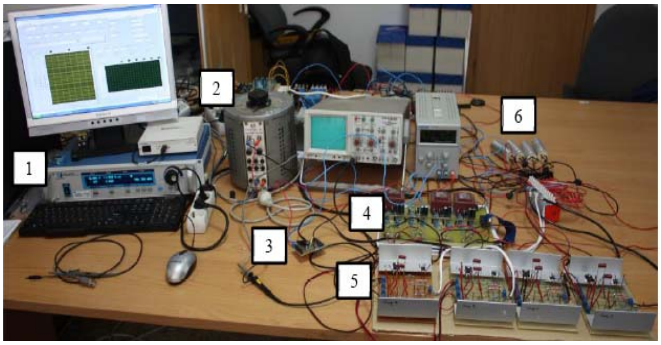

Fig. 12. The experimental setup.

The wave forms of the CCE during operation with SPIM are presented in Figure 13. The dead time was set to 1 µs.

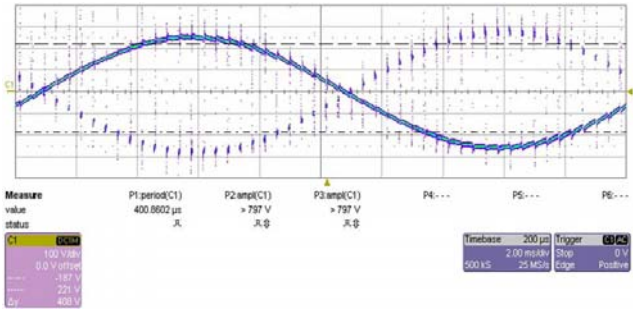

Fig. 13. The ECC voltage.

A detail is presented in Fig. 14.

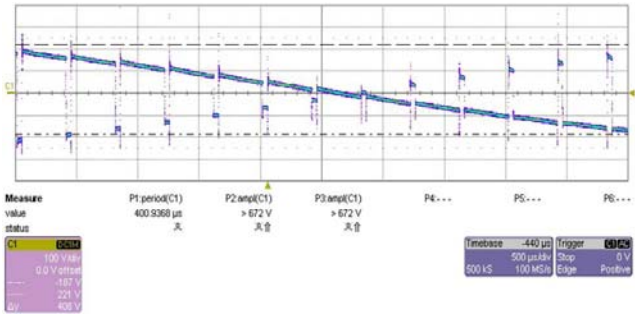

Fig. 14. The ECC voltage detail.

The experiments over control circuit have been dedicated to find the optimal frequency, over-voltages and dead time for a couple ECC-SPIM. The motor is MSP-311 model, two winding capacitor-run motor produced by *ANA IMEP Piteşti Ltd*., *Romania* designed for washing machines, with two different duty cycles: washing, at low speed (12 poles configuration), and spinning, at high speed (2 poles configuration) [18].

The aim of the experiments was to determine the optimal commutation frequency and the optimal dead-time for the given ensemble ECC-SPIM. The motor rated parameters are presented in Table 1 and Table 2.

TABLE I.

MOTOR RATED PARAMETERS

Nr.	Parameter	Unit	Value
1	Rated supply voltage	V	230
2	Rated frequency	Hz	50
3	Rated speed	rot/min	2840/420
4	Pairs of poles number	-	1/6
5	Capacitor-run value	µF	14

TABLE II.

2 AND 12 POLES CONFIGURATION PARAMETERS

Nr.	Parameter	Unit	Value
1	2 pole main winding resistance	Ω	20.8
2	2 pole auxiliary winding resistance	Ω	57.5
3	12 pole main winding resistance	Ω	73
4	12 pole auxiliary winding resistance	Ω	73
5	Cage slot number	-	40
6	Stator slot number	-	48
7	Air gap dimension	mm	.15
8	2 pole main winding turn number	-	218
9	2 pole auxiliary winding turn number	-	316
10	12 pole main winding turn number	-	1140
11	12 pole auxiliary winding turn number	-	1460

A. The optimal pulse frequency

The fixed value capacitor switching frequency in the Suciu ECC method (the same like in Lettenmaier method) is much higher than line frequency, being in the range of kHz. To establish what is the optimal pulse frequency the speed-torque characteristic has been determined in some multiple experiments in the frequency range .5 – 8 kHz. The most relevant characteristics are depicted in figure 15, the characteristics for .5, 2, 4 and 8 kHz. All others are intercalated between these four.

Being considered that the optimum means maximum torque it is obvious that the optimal value of the commutation frequency is 4 kHz.

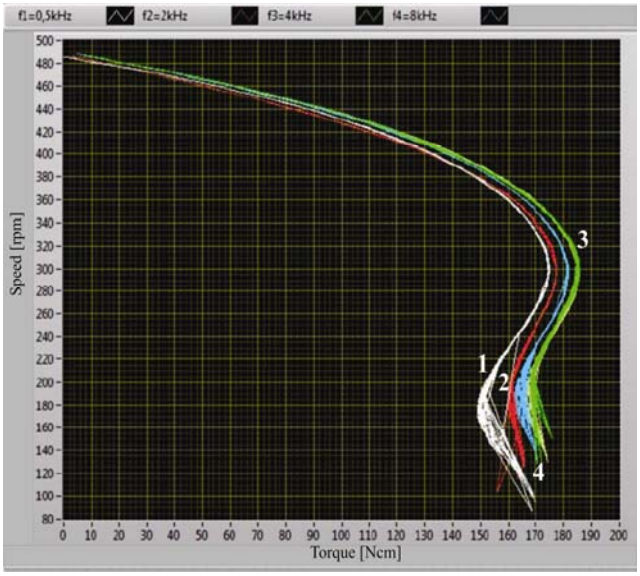

Fig. 15. The Speed/torque characteristics, 12 pole configuration and different control frequencies: white (1) - .5 kHz; red (2) - 2 kHz; green (3) - 4 kHz; blue (4) - 8 kHz.

The harmonic analyze has been revealed that the total harmonics content is lower as the switching frequency diminish. But lower switching frequency means lower maximum torque (Fig. 15) and more mechanical vibrations and noise also.

B. The motor and switches over-voltages

The Suciu ECC method has two principal drawbacks; first, the torque diminishes by about 5% and the second drawback lies in motor and switches over-voltages. There are commutation over-voltages in the range of about 50% from supply amplitude, but over-voltages from ECC principle as well [18].

A special attention in the experiments has been paid to the commutations over-voltages of the MOS-FET transistors.

In Figure 16 the transistor voltage-drop is presented. The over voltages at the switching moments are high as one may observe.

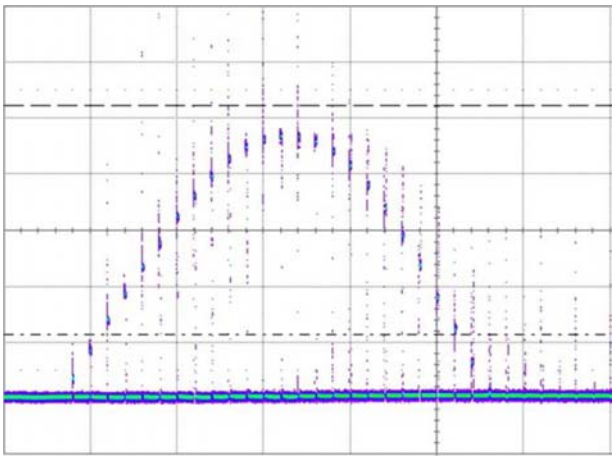

Fig. 16. The voltage drain-source of a power MOS-FET transistor from a bidirectional switch.

Some experiments have been made to establish the influence of the value of the fixed valued capacitor to the switches over-voltages. There were made in two situations, one for the minimum torque motor operation mode, the second for the rated torque operation mode. The results are presented in Fig. 17.

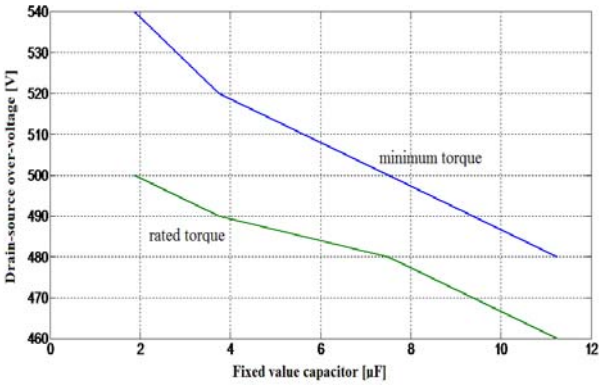

Fig. 17. The source – drain voltage of a power MOS-FET transistor from a bidirectional switch vs. the value of the fixed valued capacitor in the minimum torque motor operation mode and rated torque operation mode.

The over-voltages diminish as the capacitor value increases and, as expected in fact, they diminish with the increasing of the motor torque.

A special attention has been paid to the dead time influence. Some authors consider the dead time unavoidable, otherwise there is the danger of discharging the fixed value capacitor during the switching moments [11].

There has been analyzed the influence of the dead time over the transistor over-voltages. In Fig. 18 a comparison of the dependency between the over-voltages vs. the dead time in two cases one for the minimum torque motor operation mode, the second for the rated torque operation mode. As expected in fact, the over-voltages diminish with the dead time decrease and with the load charge increase.

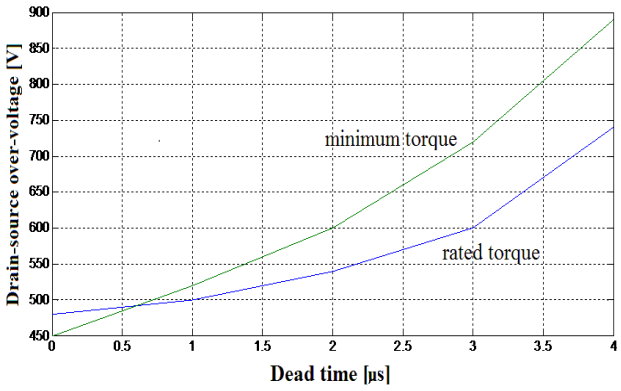

Fig. 18. The source – drain voltage of a power MOS-FET transistor from a bidirectional switch vs. the dead time of the switching pulses the minimum torque motor operation mode and rated torque operation mode.

V. Conclusions

In this paper an original control circuit for the ECC in Suciu implementation is presented.

The experiments focused on the optimization of the control pulses.

Firstly, the experiments proved that the optimum switching frequency to reach the maximum torque is 4 kHz for the ECC connected at a given SPIM. A slight advantage at lower switching frequency is the lower harmonics content, but lower frequency means more noise and mechanical vibrations.

Secondly, the over-voltages are lower as the dead time of the pulses is lower and the value of the fixed value capacitor is higher.

Thirdly, in contrast with some authors, there has been established that no dead time is the optimal solution (in this ECC case), consequently, there is no fixed value capacitor discharging at the switching moments.

Received on July 17, 2015
Editorial Approval on November 15, 2015

References

[1] T. Tudorache, L. Melcescu, "FEM optimal design of energy efficient induction machines," *Advances in Electrical and Computer Engineering,* vol. 9, no. 2, pp. 58-64, 2009.

[2] V. Ionita, L. Petrescu, A. Bordianu, O. Tabara, "Efficient use of preisach hysteresis model in computer aided design," *Advances in Electrical and Computer Engineering,* vol. 13, no. 2, pp. 121-126, 2013.

[3] I. Vlad, A. Campeanu, S. Enache, G. Petropol, "Operation characteristics optimization of low power three-phase asynchronous motors," *Advances in Electrical and Computer Engineering,* vol. 14, no. 1, pp. 87-92, 2014.

[4] G. Scutaru, A. H. Gavrila, I. Peter, "An estimation method of the manufacturing process' effect on iron losses," *Advances in Electrical and Computer Engineering,* vol. 14, no. 2, pp. 49-52, 2014.

[5] S. I. Deaconu, M. Topor, G. N. Popa, D. Bistrian, "Experimental study and comparative analysis of transients of induction motor with soft starter startup," *Advances in Electrical and Computer Engineering,* vol. 10, no. 3, pp. 27-33, 2010.

[6] E. Muljadi, Y. Zhao, T. H. Liu, T. A. Lipo, "Adjustable AC capacitor for a single-phase induction motor," *IEEE Transactions on Industry Applications*, vol. 29, no. 3, pp. 479-485, 1993.

[7] Liu, T.H.: "A maximum torque control with a controlled capacitor for a single-phase induction motor," In: *IEEE Trans. on Industrial Electronics*, Vol. 42, No. 1, February 1995, pp. 17-24;

[8] T. A. Lettenmaier, D. W. Novotny, T. A. Lipo, "Single-phase induction motor with an electronically controlled capacitor," *IEEE Transactions on Industry Applications*, vol. 52, no. 6, pp. 1564-1572, 2005.

[9] C. Suciu, M. Kansara, P.G. Holmes, W. Szabo, "Performance enhancement of an induction motor by secondary impedance control," *IEEE Transactions on Energy Conversion*, vol. 17, no. 2, pp.221-226, 2002.

[10] C. Suciu, M. Kansara, P.G. Holmes, W. Szabo, "Phase advancing for current in R-L circuits using switched capacitors," *EE Electronics Letters*, vol. 35, no. 16, pp. 1296-1297, 1999

[11] C. Suciu, L. Dafinca, M. Kansara, I. Margineanu, "Switched capacitor fuzzy control for power factor correction in inductive circuits", IEEE Power Electronics Specialists Conference, vol. 2, pp. 773-777, 2000.

[12] C. Suciu, L. Dafinca, M. Kansara, A. Szabo, "Fuzzy control of the current phase in induction circuits," 7th International Conference on Optimization of Electric and Electronic Equipment, vol. 3, pp. 631-636, 2000.]

[13] C. Suciu, L. Dafinca, R. Campeanu, "Expert phase angle control in a variable RL load circuit," 38th International Intelligent Motion

Conference; PCIM 2001 Europe, paper IM-D9, Nurnberg, Germany, 2001

[14] C. Suciu, R. Campeanu, A. Campeanu, I. Mărgineanu, A. Danila, "A virtual instrumentation-based on-line determination of a single/two phase induction motor drive characteristics at coarse start-up," IEEE-International Conference on Automation, Quality & Testing, Robotics, AQTR 2008, Cluj-Napoca, Romania, vol. 3, pp. 440-443, 2008

[15] A. Danila, I. Margineanu, R. Campeanu, C. Suciu, I. Boian, "The optimization of the single/two phase induction motor start-up with electronically switched capacitor," IEEE International Conference on Automation, Quality & Testing, Robotics, vol. 3, pp. 450-453, 2008

[16] R. Mera, R. Campeanu, "Experimental investigation of the capacitor influence on the single phase induction motor: a Labview approach," 13th WSEAS International Conference on Automation & Information, (ICAI'12), Iasi, Romania, vol. 1, pp. 184-189, 2012.

[17] R. Mera, R. Campeanu, "Optimal performance of capacitor-run single phase induction motor," 13th International Conference on Optimization of Electrical and Electronic Equipment, vol. 2, pp. 718-723, 2012.

[18] R. Campeanu, M. Cernat, "Two speed single phase induction motor with electronically controlled capacitance," *Advances in Electrical and Computer Engineering*, vol. 3, pp. 2014